

Measuring the quantum nature of light with a single source and a single detector

Gesine A. Steudle,^{1,*} Stefan Schietinger,¹ David Höckel,¹ Sander N. Dorenbos,²
 Iman E. Zadeh,² Valery Zwiller,² and Oliver Benson¹

¹*Humboldt-Universität zu Berlin, AG Nanooptik, Newtonstraße 15, 12489 Berlin, Germany*[†]

²*Kavli Institute of Nanoscience, Delft University of Technology, P.O. Box 5046, 2600 GA Delft, The Netherlands*

(Received 29 November 2011; published 15 November 2012)

An elementary experiment in optics consists of a light source and a detector. Yet, if the source generates nonclassical correlations such an experiment is capable of unambiguously demonstrating the quantum nature of light. We realized such an experiment with a defect center in diamond and a superconducting detector. Previous experiments relied on more complex setups, such as the Hanbury Brown and Twiss configuration, where a beam splitter directs light to two photodetectors, creating the false impression that the beam splitter is a fundamentally required element. As an additional benefit, our results provide a simplification of the widely used photon-correlation techniques.

DOI: [10.1103/PhysRevA.86.053814](https://doi.org/10.1103/PhysRevA.86.053814)

PACS number(s): 42.50.Ar, 42.50.Dv

The introduction of light quanta by Einstein in 1905 [1] triggered strong efforts to demonstrate the quantum properties of light directly, without involving matter quantization. It however took more than seven decades for the quantum granularity of light to be observed in the fluorescence of single atoms [2]. Single atoms emit photons one at a time; this is typically demonstrated with a Hanbury Brown and Twiss (HBT) setup [3] where light is split by a beam splitter and sent to two detectors resulting in an anticorrelation of detected events. This setup, however, evokes the false impression that a beam splitter is necessary to prove indivisibility of photons. It was already pointed out by Loudon [4] that a much simpler experiment in which the light is arranged to fall on a single phototube would be sufficient. Here, we perform such an experiment and show single-photon statistics from a quantum emitter with only one detector. The superconducting detector we fabricated has a dead time shorter than the coherence time of the emitter. No beam splitter is employed, yet anticorrelations are observed. Our work simplifies a widely used photon-correlation technique [5,6].

A single-photon Fock state is a single excitation of a mode k of the electromagnetic field $a_k^\dagger|0\rangle$. A more general single-photon state appropriate to describe the final wave packet generated by a single-photon source in an experiment is a superposition of different spatio-temporal modes containing in total one excitation. The probability $P(n)$ of finding exactly n excitations in the modes may distinguish different states of light. Figures 1(a) and 1(b) show a schematic representation of a coherent state where $P(n)$ is a Poissonian distribution together with a number (or Fock) state with exactly 1 photon per mode, respectively. In the case of a single-photon state ($n = 1$) detection of a single excitation projects the measured mode to the vacuum state; i.e., the probability of detecting another photon in the very same mode is zero. Since the temporal mode profile is associated with a characteristic coherence time τ_c , coincidence events within the time interval τ_c are absent; antibunching is observed. On the contrary,

for a coherent state the probability of detecting a photon is independent of any previous detection event. Antibunching is thus not only a consequence of photons being indivisible particles but requires a specific quantum statistical distribution of discrete excitations. The latter requirement is overlooked in a simple explanation of antibunching in a HBT experiment [Fig. 1(c)]. There a photon is regarded as a classical indivisible particle and necessarily has to decide which path to take when impinging on a beam splitter. Such an interpretation is certainly naïve. It even led to paradoxical conclusions, such as in some implementations of Wheeler's delayed choice paradox [7].

Today, many different sources have been realized that generate antibunched light such as single-photon sources based on single atoms [8,9], ions [10], molecules [11,12], color centers [13], or semiconductor quantum dots [14]. Another approach utilizes quantum correlations between photon pairs to herald the presence of a single excitation in a specific mode [15]. Photon statistics is typically measured in the above-mentioned HBT setup. However, the only reason to use a beam splitter and two detectors is to circumvent the detector's dead time. For example, commercial avalanche photodiodes (APDs) have dead times of 50 ns to 100 ns or longer, preventing the detection of coincidence events within the coherence time of typical single-photon sources, which is on the order of a few nanoseconds. Although more recent experiments could generate single photons with coherence times up to several microseconds [16–18] HBT setups are still used. Placing two detectors in the spatial mode of the photon flux, the beam splitter is not required any more, but still the photons are “split” to either of the detectors at different locations [19].

Recently, measurements of photon statistics with single detection devices based on a gated Geiger mode InGaAs APD [20] or a modified streak camera in single-photon counting mode [21,22] were reported. Nonclassical dynamic features were observed in the light from semiconductor microlasers. However, it was so far not possible to detect nonclassical properties of light from a single quantum emitter [23] because of poor detection efficiency.

In our approach, we determine the statistical properties of a photon stream from a single emitter by detecting the arrival times of individual photons with a single detector [Fig. 1(d)].

* steudle@physik.hu-berlin.de

[†] <http://www.physik.hu-berlin.de/nano>

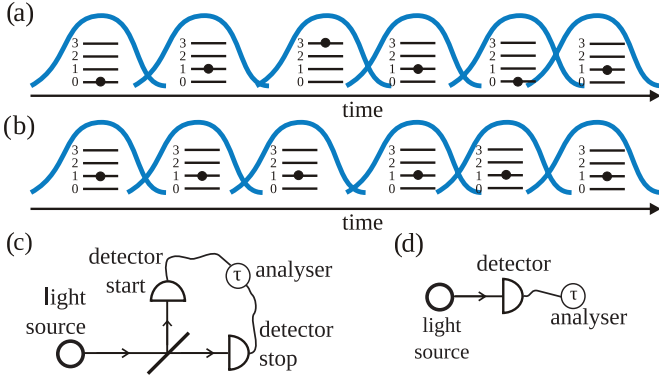


FIG. 1. (Color online) Cartoon of a coherent state (a) and a single-photon Fock state (b). Spatial-temporal modes (indicated by lines) of a specific coherence time are populated by discrete excitations. For a coherent state this image corresponds to a snapshot, since the number of excitations per mode n can only be predicted with a certain probability $P(n)$. In a single-photon Fock state there is exactly one excitation per mode. A detection event projects the mode to the vacuum state. (c) Schematics of a standard Hanbury Brown and Twiss setup, where the light is split on a beam splitter allowing intensity correlation measurements within time intervals shorter than the individual detector dead times. (d) Direct statistical analysis of light by detecting single-photon arrival times with a single detector.

For this, the detector's dead time τ_d has to be shorter than the characteristic correlation time. In the case of weak excitation this correlation time is the Fourier-limited coherence time τ_c of the photons corresponding to the lifetime τ_{life} of the excited state, so we require $\tau_d < \tau_{\text{life}}$. In our experiment we use a nitrogen-vacancy (N-V) center in diamond [24] as a single-photon source together with a superconducting single-photon detector (SSPD).

In the N-V center in diamond a nitrogen atom replaces a carbon atom with an adjacent vacancy in the diamond lattice. N-V centers are the subject of intense research due to their exceptional role as single-photon sources at room temperature. The optical transition in a N-V center occurs between two spin-triplet states. At least one additional singlet state introduces an off-state. The fluorescence spectrum of a N-V center is broadened by higher phonon lines, but has a pronounced zero phonon line peak at 638 nm. At room temperature, single-photon emission with count rates up to 10^6 s^{-1} can be observed [25]. The lifetime of the excited state in N-V centers in diamond nanoparticles is around 30 ns, which is long compared to other single-photon sources [26].

As a single-photon detector, we utilized a fiber-coupled SSPD [27]. It consists of a 100 nm wide and 5 nm thick NbN meandering nanowire entirely fabricated at TU Delft, which covers an area of $10 \mu\text{m} \times 10 \mu\text{m}$ with a fill factor of 50% coupled to a single-mode fiber glued on the back side of the sapphire substrate, which was for that purpose thinned to 100 μm and polished [Fig. 2(a)]. The detector chip is mounted on a dipstick immersed in liquid helium (4.2 K) and biased at 90% of its critical current. The pulses from the detector are amplified by 76 dB with two 2 GHz bandwidth amplifiers (minicircuits) and fed to an oscilloscope with 1 GHz bandwidth. The dark count rate of the detector was $< 50 \text{ s}^{-1}$ and its overall efficiency at 630 nm was around 10%. Its dead

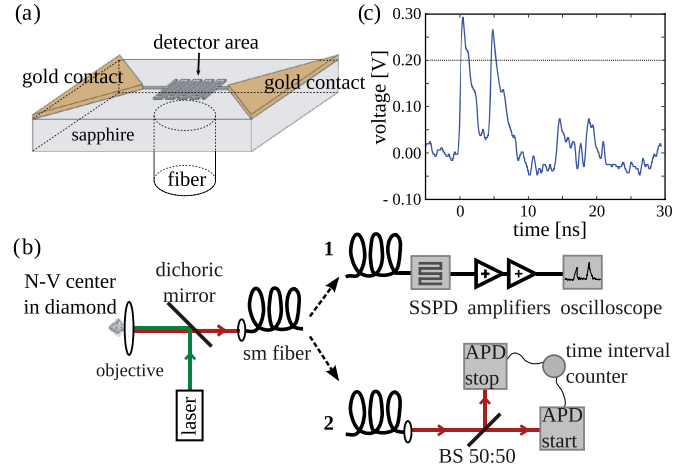


FIG. 2. (Color online) Experimental setup. (a) Scheme of the fiber-coupled detector chip. (b) A single N-V center in a diamond nanocrystal is excited with a 532 nm cw laser. Its emission is collected via a confocal optical microscope, coupled to a single mode (sm) optical fibre, and detected in two configurations: (1) a single fiber-coupled SSPD and (2) a standard free beam Hanbury Brown–Twiss (HBT) setup containing a beam splitter (BS) and two avalanche photodiodes (APDs). Correlations are analyzed by a fast 1 GHz oscilloscope or by a time interval counter. (c) Typical voltage trace with two detection events recorded with the oscilloscope. Only double events with a time difference of between 5 ns and 200 ns were collected.

time is limited by its kinetic inductance [28], here $\tau_d < 5$ ns. Yet, this value is clearly shorter than the N-V center's lifetime. Antibunching is quantified by measuring the second-order autocorrelation function of the electric field, given by

$$g^{(2)}(\tau) = \frac{\langle : I(t)I(t+\tau) : \rangle_t}{\langle I(t) \rangle_t^2}, \quad (1)$$

where $I = E^\dagger E$ is the field intensity and $: :$ denotes normal ordering. For uncorrelated light, e.g., laser light, with a Poissonian photon number distribution, $g^{(2)}(\tau) = 1$ for all τ . However, for a number state $|n\rangle$, at $\tau = 0$ it drops to $g^{(2)}(0) = 1 - 1/n < 1$.

Figure 2(b) shows the experimental setup for measuring the $g^{(2)}$ function. The fluorescence was coupled into a single-mode fiber, and detection was done in two configurations. Configuration 1 is the single-detector setup; i.e., the light was sent via the optical fiber directly to the SSPD. In configuration 2, the HBT setup, light was coupled for comparison into a standard free space HBT setup consisting of a beam splitter and two APDs. In configuration 1, the amplified electrical pulses from the SSPD were fed to an oscilloscope (Tektronix DPO 7104, pinpoint-trigger mode) with 1 GHz bandwidth. The oscilloscope was programmed to save a pulse trace whenever a trigger level of 200 mV was exceeded twice with a time difference between 5 ns and 200 ns [see Fig. 2(c)]. To measure the $g^{(2)}$ function, 30 000 traces were recorded and analyzed. The $g^{(3)}$ and higher correlations are readily obtained from the same measurement. In configuration 2, the time intervals between signals from the two APDs were recorded with a time interval counter.

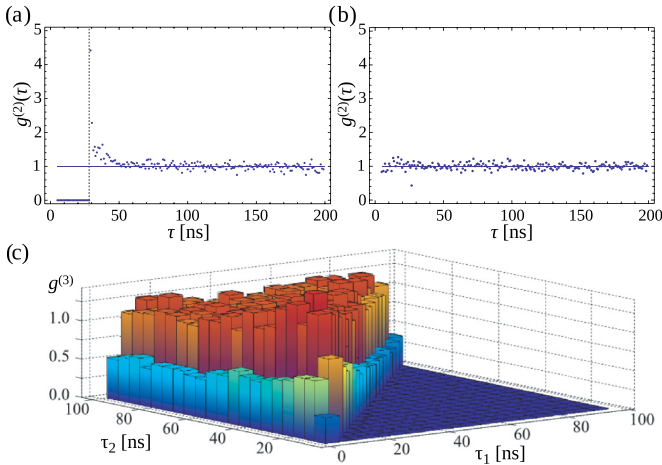


FIG. 3. (Color online) Correlation measurements with classical light. (a) Measured $g^{(2)}$ function of an attenuated laser beam sent to a single commercial APD and analyzed via the fast oscilloscope by evaluating traces when a second detection event occurs within a time window of 5 ns to 200 ns. The dashed line indicates the APD dead time. The bunching observed between correlation times of 30 ns and 50 ns is due to afterpulsing. For a rate of $300\,000\text{ s}^{-1}$ and an afterpulsing probability of 0.5% one out of eleven events is an afterpulsing event and contributes to the area above the solid line [$g^{(2)}(\tau) = 1$]. (b) Same measurement, but with a SSPD with a dead time shorter than 5 ns. Since only time differences larger than 5 ns were recorded no dead time effect was resolved. The absence of any correlation indicates a Poissonian photon number distribution. The solid line is a linear fit. (c) $g^{(3)}$ function from an attenuated laser beam measured with a single SSPD obtained by analyzing oscilloscope traces containing 3 or more detection events; τ_1 and τ_2 are the time intervals between detection events. The 4 ns dead time of the detector yields the expected flat $g^{(3)}$ function for times longer than 5 ns. Bin sizes are 1 ns for the $g^{(2)}$ measurements and 5 ns for the $g^{(3)}$ measurement.

We first performed two test experiments with classical light. Light from an attenuated laser was coupled into only one of the APDs and the detector clicks were fed into the oscilloscope. The measured $g^{(2)}$ function [Fig. 3(a)] shows the absence of coincidence counts at time intervals shorter than 30 ns. This is due to the dead time of the APD preventing detection of coincidence events within a 30 ns time interval. It is interesting to note the similarity of this classical suppression of coincidences compared to antibunching where the suppression is due to the quantum mechanical projection of a quantum state. For correlation times between 30 ns and 50 ns a bunching feature is observed due to the APD's afterpulsing. The afterpulsing probability according to the manufacturer is 0.5%. Here this is relevant since at our photon count rates of around $300\,000\text{ s}^{-1}$ the probability for a second photon to arrive within a time window between 30 ns and 200 ns after a first one is 5%; i.e., one out of eleven events when a second pulse is detected is due to afterpulsing. These events account for the bunching observed in Fig. 3(a). In a second test we coupled attenuated laser light into the SSPD and again measured the $g^{(2)}$ function [Fig. 3(b)]. Obviously, there are no correlations among incoming photons and, more important, no suppression of coincidence events in the time window

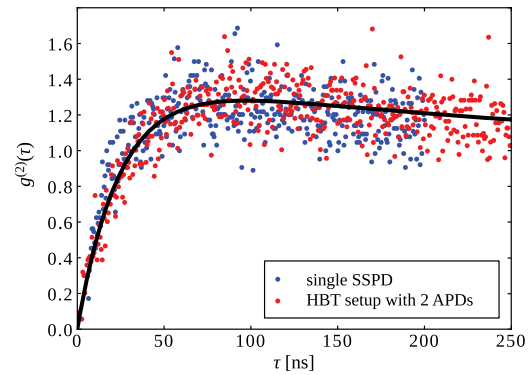


FIG. 4. (Color online) Antibunching measured with a single detector. Measurement of the $g^{(2)}$ function in the single-detector configuration 1 of Fig. 2(b) [blue (dark grey) dots] and the standard HBT configuration, configuration 2 of Fig. 2(b) [red (light grey) dots], respectively. The black line is a fit to a three-level rate equation model. An additional bunching is observed due to occasional population of a metastable singlet state.

of interest (5 ns to 200 ns). Furthermore, no afterpulsing is observed. Since the intensity autocorrelation signal is constant after 5 ns, we can conclude that this is an upper limit for the dead time of our SSPD. Analyzing oscilloscope traces with 3 or more detection events enabled the construction of the $g^{(3)}$ function presented in Fig. 3(c). Our $g^{(3)}$ values are measured correlations in 3 different space-time points. The coincidence data are extracted from time-tagged arrivals of photons on the detector. This is comparable to the work by Höckel *et al.* [29] and Elvira *et al.* [30].

Finally, a nanodiamond sample was prepared by spin-coating an aqueous suspension of nanodiamonds onto a glass coverslip. Typical heights between 20 and 35 nm are found for the nanodiamonds while the lateral extension is up to twice these values. Only around 1% of them contain a single N-V center. Such a single center was located using an inverted microscope as described elsewhere [31]. The 532 nm continuous wave excitation light was filtered out before coupling the emission into a single-mode optical fiber. We measured the $g^{(2)}$ function in the two different configurations of Fig. 2(b), the single-detector setup (configuration 1) and the standard HBT setup (configuration 2). The experimental results are shown in Fig. 4. Blue (dark grey) dots correspond to the $g^{(2)}$ function measured with the single SSPD. It has a pronounced antibunching dip which fits well to a three-level rate equation model (solid black line). Red (light grey) dots correspond to the standard HBT measurement.

Obviously, both measurements shown in Fig. 4 reveal the quantum nature of the photon stream in the same manner, proving that a statistical analysis of a stream of single photons can very well be performed with a single detector only. Our results highlight the fact that the nonclassicality of light appears even in a most elementary experiment without the need to introduce additional optical elements, such as a beam splitter dividing photons or a second detector. A single fast detector with a short dead time can provide the same statistical information as a standard HBT setup with two detectors. Fast

detection of single photons is highly attractive to determine higher order correlation functions $g^{(n)}$ [see for example Fig. 3(c)] or to study more complex nonclassical photon states, such as superpositions of different modes in the temporal rather than in the spectral [32] or spatial [33] domain. Antibunching from sources with shorter coherence times can be measured by further reducing the detector dead time which is here limited by its kinetic inductance. For example shortening the wire or using a parallel meander geometry are possible routes [34]; we present in the Appendix two detection events separated by 2.7 ns using an SSPD designed for reduced dead time. Finally, even beyond fundamental considerations such detectors are useful to enable the single-detector scheme in fluorescence correlation spectroscopy [5] on shorter time scales than were possible previously.

We acknowledge financial support by the German Research Foundation, DFG (SFB 787), the Federal Ministry of Education and Research, BMBF (KEPHOSI), the Foundation for Fundamental Research on Matter, FOM, and the Netherlands Organization for Scientific Research, NWO (VIDI). Valuable discussions with Ulrike Herzog are acknowledged.

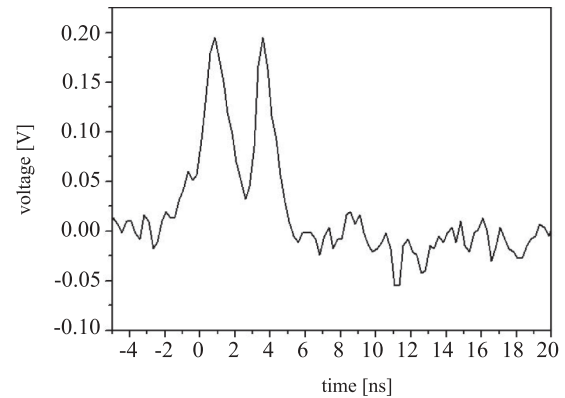


FIG. 5. Two detection events separated by 2.7 ns measured on a specially designed SSPD with reduced dead time.

APPENDIX

Using our SSPDs, a second photon can be detected before the first detection pulse has completely decayed, as shown in Fig. 5. For the correlation measurements, however, a minimum pulse separation of 5 ns was chosen to prevent artifacts.

-
- [1] A. Einstein, *Ann. Phys.* **17**, 132 (1905).
- [2] H. J. Kimble, M. Dagenais, and L. Mandel, *Phys. Rev. Lett.* **39**, 691 (1977).
- [3] R. Hanbury Brown and R. Q. Twiss, *Nature (London)* **177**, 27 (1956).
- [4] R. Loudon, *The Quantum Theory of Light* (Oxford University Press, Oxford, 1973).
- [5] P. Schwille, *Cell. Biochem. Biophys.* **34**, 383 (2001).
- [6] P. Kok, W. J. Munro, K. Nemoto, T. C. Ralph, J. P. Dowling, and G. J. Milburn, *Rev. Mod. Phys.* **79**, 135 (2007).
- [7] V. Jacques, E. Wu, F. Grosshans, F. Treussart, P. Grangier, A. Aspect, and J.-F. Roch, *Science* **315**, 966 (2007).
- [8] P. Grangier, G. Roger, and A. Aspect, *Europhys. Lett.* **1**, 173 (1986).
- [9] F. Diedrich and H. Walther, *Phys. Rev. Lett.* **58**, 203 (1987).
- [10] H. G. Barros, A. Stute, T. E. Northup, C. Russo, P. O. Schmidt, and R. Blatt, *New J. Phys.* **11**, 103004 (2009).
- [11] R. Brouri, A. Beveratos, J.-P. Poizat, and P. Grangier, *Phys. Rev. A* **62**, 063817 (2000).
- [12] K. G. Lee, X. W. Chen, H. Eghlidi, P. Kukura, R. Lettow, A. Renn, V. Sandoghdar, and S. Götzinger, *Nat. Photonics* **5**, 166 (2011).
- [13] C. Kurtsiefer, S. Mayer, P. Zarda, and H. Weinfurter, *Phys. Rev. Lett.* **85**, 290 (2000).
- [14] P. Michler, A. Kiraz, C. Becher, W. V. Schoenfeld, P. M. Petroff, L. Zhang, E. Hu, and A. Imamoglu, *Science* **290**, 2282 (2000).
- [15] C. K. Hong and L. Mandel, *Phys. Rev. Lett.* **56**, 58 (1986).
- [16] H. P. Specht, J. Bochmann, B. W. M. Mücke, E. Figueroa, D. L. Moehring, and G. Rempe, *Nat. Photonics* **3**, 469 (2009).
- [17] M. Scholz, L. Koch, and O. Benson, *Phys. Rev. Lett.* **102**, 063603 (2009).
- [18] J. S. Neergaard-Nielsen, B. M. Nielsen, H. Takahashi, A. I. Vistnes, and E. S. Polzik, *Opt. Express* **15**, 7940 (2007).
- [19] E. A. Dauler, M. J. Stevens, B. Baek, R. J. Molnar, S. A. Hamilton, R. P. Mirin, S. W. Nam, and K. K. Berggren, *Phys. Rev. A* **78**, 053826 (2008).
- [20] A. R. Dixon, J. F. Dynes, Z. L. Yuan, A. W. Sharpe, A. J. Bennett, and A. J. Shields, *Appl. Phys. Lett.* **94**, 231113 (2009).
- [21] J. Wiersig, C. Gies, F. Jahnke, M. Assmann, T. Berstermann, M. Bayer, C. Kistner, S. Reitzenstein, C. Schneider, S. Höfling, A. Forchel, C. Kruse, J. Kalden, and D. Hommel, *Nature (London)* **460**, 245 (2009).
- [22] M. Assmann, F. Veit, M. Bayer, M. van der Poel, and J. M. Hvam, *Science* **325**, 297 (2009).
- [23] M. Assmann, F. Veit, J.-S. Tempel, T. Berstermann, H. Stolz, M. van der Poel, J. M. Hvam, and M. Bayer, *Opt. Express* **18**, 20229 (2010).
- [24] F. Jelezko and J. Wrachtrup, *Phys. Status Solidi A* **203**, 3207 (2006).
- [25] T. Schröder, F. Gädeke, M. J. Banholzer, and O. Benson, *New J. Phys.* **13**, 055017 (2011).
- [26] P. Michler, *Single Semiconductor Quantum Dots* (Springer, Berlin, 2009).
- [27] G. N. Gol'tsman, O. Okunev, G. Chulkova, A. Lipatov, A. Semenov, K. Smirnov, B. Voronov, A. Dzardanov, C. Williams, and R. Sobolewski, *Appl. Phys. Lett.* **79**, 705 (2001).
- [28] A. J. Kerman, E. A. Dauler, W. E. Keicher, J. K. W. Yang, K. K. Berggren, G. Gol'tsman, and B. Voronov, *Appl. Phys. Lett.* **88**, 111116 (2006).

- [29] D. Hockel, L. Koch, and O. Benson, *Phys. Rev. A* **83**, 013802 (2011).
- [30] D. Elvira, X. Hachair, V. Verma, R. Braive, G. Beaudoin, I. Robert-Philip, I. Sagnes, B. Baek, S. W. Nam, E. A. Dauler, I. Abram, M. J. Stevens, and A. Benveratos, arXiv:1106.1279.
- [31] S. Schietinger, M. Barth, T. Aichele, and O. Benson, *Nano Lett.* **9**, 1694 (2009).
- [32] P. J. Mosley, A. Christ, A. Eckstein, and C. Silberhorn, *Phys. Rev. Lett.* **103**, 233901 (2009).
- [33] S. B. Papp, K. S. Choi, H. Deng, P. Lougovski, S. J. van Enk, and H. J. Kimble, *Science* **324**, 764 (2009).
- [34] E. Dauler, B. Robinson, A. Kerman, J. Yang, E. Rosfjord, V. Anant, B. Voronov, G. Gol'tsman, and K. Berggren, *IEEE Trans. Appl. Supercond.* **17**, 279 (2007).